Electrical and magnetic properties of UFe$_x$ compounds

E. Verdín

Programa de Posgrado en Ciencias (Física) Universidad de Sonora,
Calle Rosales y Boulevard Luis Encinas, 83000 Hermosillo, Son., México

R. Escudero

Instituto de Investigaciones en Materiales, Universidad Nacional Autónoma de México,
Apartado Postal 70-360, 04510 México, D.F., México.

UFe$_x$ alloys with compositions from x = 1.60 to 13.20 at. % of Fe, are superconducting with maximum transition temperature, Tc = 3.59 K. X-ray diffraction analysis, shows the existence of different compositions with formula α-U+Fe and solubility limit close to x = 1.76 $\pm$ 0.87 at. % Fe. With increasing Fe the solid solution U$_6$Fe phase forms and coexists with the metastable α-U+Fe until it saturates. The annealing process to the samples accelerates the formation of U$_6$Fe, modifying substantially the magnetic characteristics, but without changing its superconducting transition.

Keywords: Superconductivity; Magnetism; Heavy Fermions; U alloys.

Aleaciones de UFe$_x$ con composiciones desde x = 1.60 a 13.20 (at. % de Fe) muestran transiciones superconductoras que se incrementan hasta una temperatura máxima de T$_C$ = 3.59 K. Análisis de difracción por rayos X muestran la formación de diferentes composiciones α-U+Fe, con límite máximo de saturación cercano a x$_{sat}$ = 1.76 $\pm$ 0.87 at. % Fe. En x$_{sat}$ se inicia la formación de la solución sólida U$_6$Fe. El recocido de las muestras incrementa la formación de U$_6$Fe, a expensas de las composiciones metaestables iniciales. Este proceso de recocido modifica substancialmente las características magnéticas de las composiciones intermedias, pero sin que cambien las características superconductoras.

Descriptores: Superconductividad; magnetismo; fermiones pesados; aleaciones de uranio.

PACS: 74.70.Ad; 74.25.Ha; 74.70.Tx

1. Introduction

Actinides and lanthanides elements with incomplete f-shells present many interesting characteristics when alloyed with transition metals. Uranium element, for instance, has an incomplete electronic f-shell and is paramagnetic and superconducting near 0.68 K [1-2]. It can give rise to heavy fermion behavior with superconducting, antiferromagnetic, ferromagnetic, and paramagnetic characteristics when alloyed with transition elements. Heavy fermion behavior arises because the f-electronic shell, being incomplete and ill-formed, is relatively close to the Fermi level and at low temperatures it may resonates, mixing the d band and f electrons. The result of this process is a compound in which the mass of the electrons may be one or two orders of magnitude bigger than the free electronic mass. This enhanced electronic mass is readily noted in specific heat measurements at low temperatures. Resistivity and magnetic measurements as function of temperature also show the anomalous non-fermi liquid behavior characteristic of a heavy fermion compound.

The intermetallic uranium alloys U$_6$Fe and UFe$_2$, have already been studied by other authors [2-14]. U$_6$Fe, solid solution presents superconductivity with heavy fermion characteristics at 3.86 K [6,7,11], whereas UFe$_2$ is a ferromagnet with Curie temperature about 195 K according to Komura, *et al.* [12], Gordon found 151 K [13], and Lin and Ogilvie [14] reported 172 K, which indicate that the change in the Curie temperature depends of either the purity of the elements or preparation method. Other alloys with Fe and U with composition U$_7$Fe, U$_5$Fe [9], and UFe$_x$ with x = 0 to 1.3 at. % Fe [5], have been studied.

In this paper we report our studies on the superconducting and magnetic behavior of compositions UFe$_x$, with x from 1.60 to 13.2 at. % Fe.

2. Experimental procedure

Polycrystalline buttons of different UFe$_x$ compositions were obtained using a radio-frequency induction furnace (RF), provided with water-cooled cooper crucible. Uranium metal was purified by a re-melting process under argon atmosphere [15,16], with this process we obtained purities of about 99.5 % checked by electron microanalysis with resolution of 100 nm, and accuracy of about 1%. Iron shots, purities about 99.999 % (Aldrich) were used. Appropriate amounts of the two components were melted together several times (at least six times) in order to assure good homogeneity. The melting was performed in argon atmosphere (99.99 %). The resulting compositions were quenched from the RF oven by turning off the power; the Cu crucible acts as heat sink. The annealed process was carried out wrapping the sample in tantalum foil, sealed in quartz tubes, and heated for one day at 720 ^{o}C, and for two days at 600 ^{o}C.

With electron-probe microanalysis we examine the samples; it reveals that the as-casting samples were homogeneous in all six compositions. The Fe content was 1.60, 2.67, 3.67,
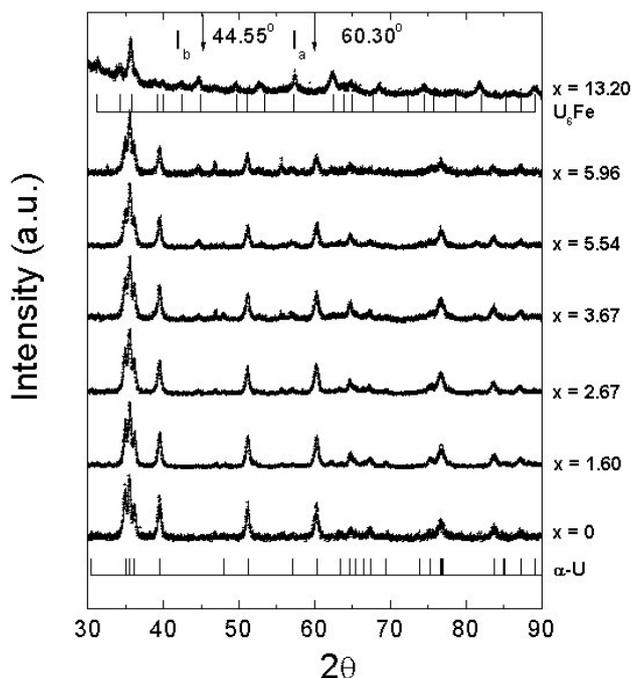
5.54, and 5.96, to 13.20 at. %. The annealed samples showed small amounts of uranium precipitates in the region of compositions, between U_6Fe and pure uranium. In Fig. 1 we present the zone of formation for the UFe$_x$ from the phase diagram by Okamoto [3]. It shows maximum solubility of about 2 % Fe in uranium. The inset of the same figure shows the complete phase diagram.

Powder diffraction data (XRD) were measured at room temperature in a Siemens D5000 diffractometer, with CuK$_\alpha$ radiation, and scanning speed of 0.3 degree/min from 15°

to 90°. Rietveld refinements were performed using the RietQuan software [17].

Resistance versus temperature measurement were performed from 1.8 K to 300 K in a quantum design PPMS facility with the standard four copper wires attached to the specimen with silver paint. Magnetic measurements were carried out in a quantum design SQUID magnetometer at zero field cooling (ZFC) and field cooling (FC) modes, from 1.8 K to 300 K using low magnetic fields (10 Oe).

FIGURE 1. U-Fe phase diagram, by Okamoto [3].

FIGURE 2. Diffraction patterns (crosses) and Rietveld refinements (solid line) of six UFe$_x$ samples. The arrows indicate the position of selected peaks, as explained in the text. The percentage of Fe, is shown. Data for α-U and U$_6$Fe are included.
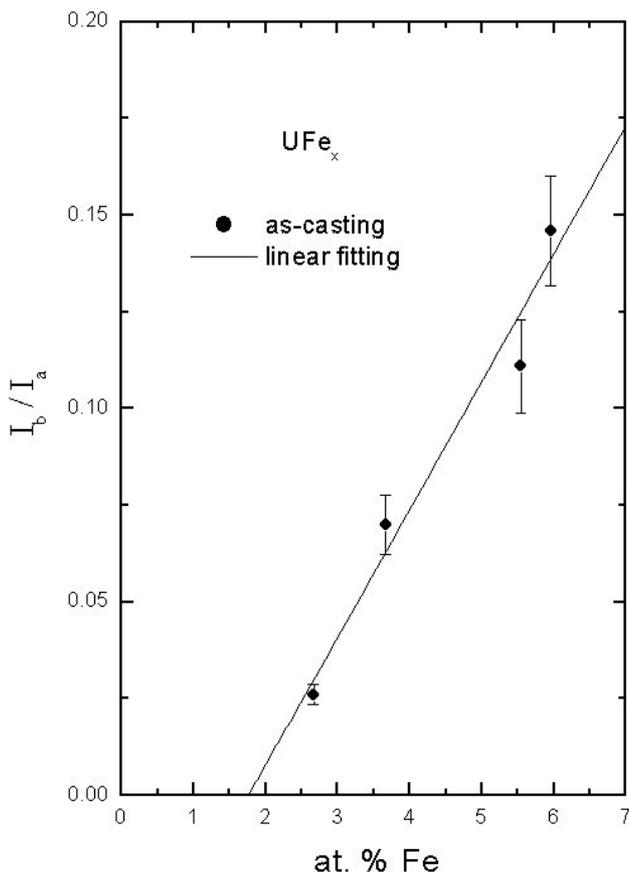

FIGURE 3. The ratio of intensities I$_b$/I$_a$ for as-casting alloys at different at. % of Fe. The solid line is a linear fit.

3. Results and discussion

X-ray diffraction patterns for the as-casting samples for α-U, intermediate compositions, and U$_6$Fe (x = 13.20) are shown in Fig. 2. For comparison, we used published files by the International Center for Powder Diffraction Data as vertical lines. Rietveld refinements (solid line) performed for compositions between 0.0 and 1.60 at. % of Fe are almost identical and agree well with α-uranium data. For the higher composition with x = 13.20, the data is in agreement with U$_6$Fe [9]. We see in Fig. 2, that when the iron content is increased, for concentrations above x = 1.60 %, U$_6$Fe peaks ($2\theta = 44.55°$) start to be notorious and increase their intensity. At that moment, the intensities of α-U peaks ($2\theta = 60.30°$) start to decrease, manifesting the coexisting of two phases. To establish the approximate limits between these two phases [18], we utilized the intensities of two unambiguous peaks without interference of adjacent peaks; one at $2\theta = 44.55°$, belonging to U$_6$Fe and other at $2\theta = 60.30°$, that belongs to α-uranium. The ratio of intensities between the first peak, denoted as (I$_b$) and the second one denoted as (I$_a$), versus the % of Fe in U is plotted in Fig. 3. Linear fitting (solid line), permit us to conclude, that U$_6$Fe phase is negligible below 1.76 ± 0.87 at. % Fe, within the X-ray diffraction resolution (assumed ~5 %), and also in accord to the phase diagram.

Normalized resistance, R(T)/R(240 K) as function of temperature, from 1.8 to 4 K for the as-casting samples, is presented in Fig. 4. The result shows that when iron increases, the slope of the resistance curves increases, and the system becomes superconducting at about 1.60 at. % Fe. The critical superconducting temperature, increase up to ~3.59 K for 13.20 at. % Fe (for more details, see Table I). Note that this sample displays a normalized resistance bigger than other compositions, which might be due to heavy fermion behavior of the U$_6$Fe. Figure 5 shows R(T)/R(240 K) curves for the annealed samples. In this set of samples, we noted that R=0 is reached at 3.67 at. % Fe, and Tc decreases for higher compositions. Tc's, for the as-casting and annealed samples, for each Fe content are included in Table I. It is important to mention that the overall resistive behavior of the two families of samples (as-casting and annealed) measured from 4 K to 240 K, show notorious differences; whereas the as casting samples present metallic behavior, the annealed ones present a noticeable deviation from linearity from 60 to 90 K [16].

Magnetization measurements M(T) performed in samples with and without annealing, at 10 Oe, and at ZFC and FC modes from 1.8 to 4.0 K, are presented in Figs. 6 and 7, respectively. These measurements confirm the existence of superconductivity in both sets of samples. For more information about the superconducting behavior, the Meissner fraction was determined for the two sets of samples, the values are included in Table I. As we may see, the Meissner fraction is increased for the annealed samples. Figure 8 shows the magnetization in ZFC and FC modes, with applied magnetic

TABLE I. Critical temperatures determined by R - T and M - T measurements, and the Meissner fraction for different compositions of Fe in UFe$_x$ alloys

at. % Fe	R - T as-casting Tc (K)	R - T annealed Tc (K)	M - T as-casting Tc (K)	M - T annealed Tc (K)	Meissner fraction as-casting	Meissner fraction annealed
1.60	2.78	—	2.72	2.50	0.08	0.79
2.67	3.17	2.96	2.87	2.85	0.72	3.31
3.67	3.43	3.19	3.21	3.15	0.80	3.37
5.54	3.35	3.25	3.04	3.24	0.57	5.13
5.96	3.37	3.42	3.14	3.35	0.52	6.98
13.20	3.59	3.48	3.44	3.27	15.45	6.80

FIGURE 4. Normalized resistance at low temperature for as-casting alloys at different percentages of Fe.

FIGURE 5. Normalized resistance at different at. % of Fe for annealed samples as function of temperature.

field of 10 Oe for the annealed samples between 5 K and room temperature. In the FC mode we observed that a spontaneous magnetization occurs at about 175 K. This has the signature of a ferromagnetic transition [4,7]. However, the important fact is that magnetic ordering does not destroy superconductivity, as observed when the low temperature region is reached.

According to the previously results, we can conclude that a solid solution of U-Fe compositions can be formed with different Fe content. It is found that the solubility of iron in uranium is small, but has not been completely determined so far.
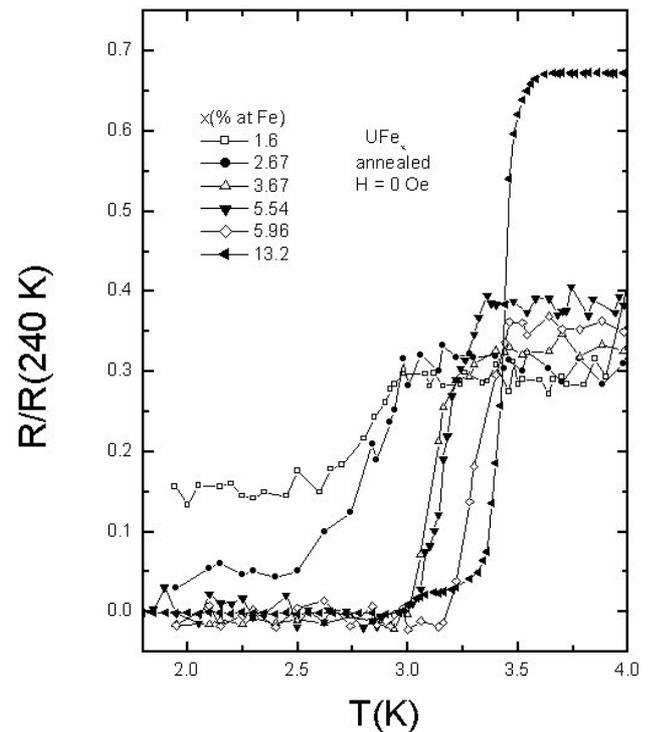
However this work opens the possibility that γ-U in γ-Fe and α-Fe alloys can be found at higher concentrations. The phase equilibrium diagram of U- Fe needs further study. Going back to Fig. 3, it is possible to see that the as-casting samples present two phases, UFe$_x$ and U$_6$Fe. The first one is a solid solution with the maximum solubility at 1.76 ± 0.87 at. %Fe, see the doted vertical line in Fig. 1. The second phase is formed in the peritectic line (810 °C) at 14.28 at. % Fe.

Transport and magnetic measurements show that all alloys are superconducting below 3.59 K. The transition temperatures increases from 0.6 K (α-U) to below 3.86 K (U$_6$Fe).
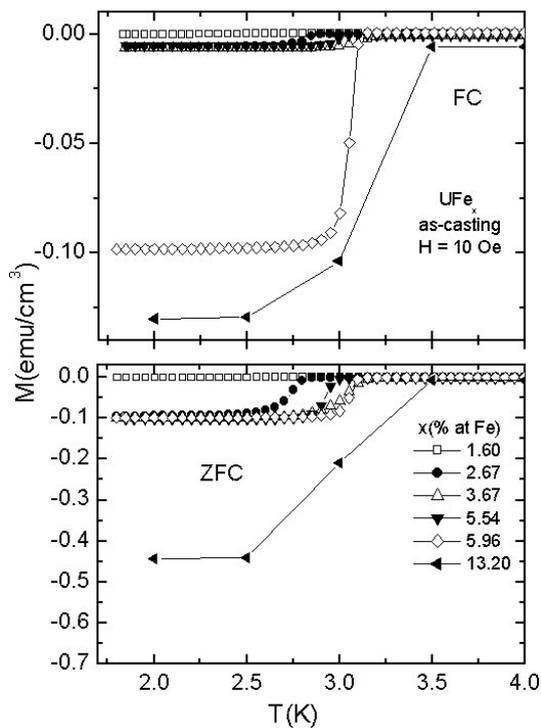
FIGURE 6. Magnetization versus Temperature, for different at. % of Fe, measured at low magnetic field (10 Oe.), for as-casting samples. ZFC and FC modes are displayed.
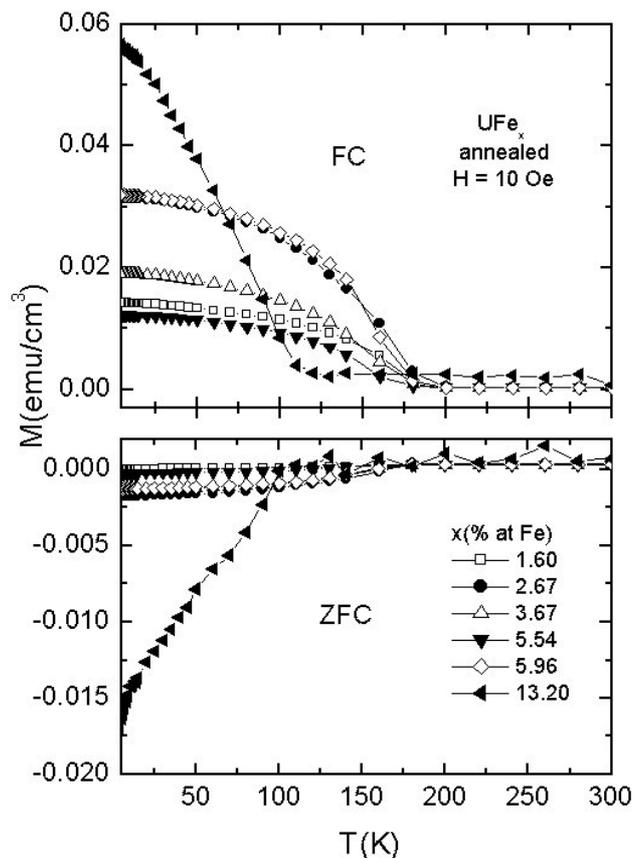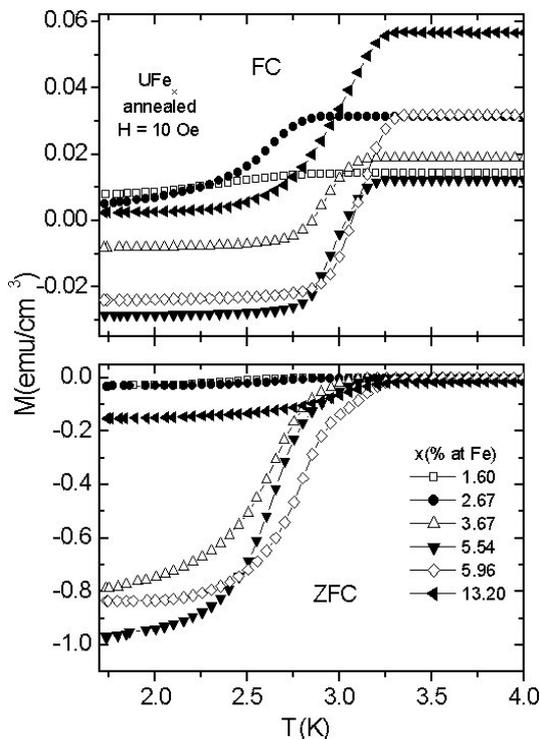

FIGURE 7. Magnetization versus Temperature, for different at. % of Fe, measured at a magnetic field (10 Oe.), for annealed samples. ZFC and FC modes are displayed.

FIGURE 8. Magnetization versus Temperature at FC and ZFC modes for annealed samples.

Once the alloys are annealed they are ferromagnetic, without changing the superconducting temperature, but with magnetic ordering onset below 200 K. Some authors [4,7] attribute part of this effect to magnetic impurities of UFe_2, and to the strong paramagnetism of the U_6Fe. Nevertheless the behavior observed of Tc as function of x in Table I, is unusual for this binary alloy [19], close similarity was observed in $TiFe_x$ and $TiCo_x$ [20], where the 3d magnetic transition elements (Fe, and Co) increase the superconducting temperature by an order of magnitude. In closing, it is interesting to observe as a result of this study, that the Meissner fraction increased with the magnetic ordering. We conclude that the coexistence of the two phenomena that in BCS superconductors are excluded brings the possibility to study new forms of paring condensation beyond BCS theory.

Acknowledgements

1. R.A. Hein, W.E. Henry, and N.M. Wolcott, *Phys. Rev.* **107** (1957) 1517.

2. L.F. Bates and J.R. Mallard, *Proc. Phys. Soc. London*, sec. B **63** (1950) 520.

3. H. Okamoto, *Phase Diagrams of Binary Iron Alloys* (Monograph Series on Alloy Phase Diagrams, ASM International) (1987) p. 429.

4. L.E. DeLong, R.P. Guertin, S. Hasanain, and T. Fariss, *Phys. Rev. B* **31** (1985) 7059.

5. N. Swindells, *J. Nucl. Mater*, **18** (1966) 261.

6. E. Yamamoto, M. Hedo, Y. Inada, T Ishida, Y. Haga, and Y. Onuki, *J. Phys. Soc. Japan* **65** (1996) 1034.

7. E. Yamamoto, Y. Haga, A. Nakamura, N. Kimura, Y. Inada, H. Sugawara, H. Sato, and Y. Onuki, *Physica B* **230-232** (1997) 394.

8. J.J. Engelhardt, *J. Phys. Chem. Solids*, **36** (1975) 123.

9. R. W.White, J.D.G. Lindsay, and R.D. Fowler, *Solid State Commun.* **13** (1973) 531.

10. A.P. Goncalves, H. Noel, J.C. Waerenborgh, *J. Magn. Magn. Mater.* **251** (2002) 1.

11. L.E. DeLong, J.G. Huber, K.N. Yang, and M.B. Maple, *Phys. Rev. Lett.* **51** (1983) 312.

12. S. Komura, N. Kunitomi, Y. Hamaguchi, and M. Sakamoto, *J. Phys. Soc. Japan* **16** (1961) 1486.

13. P. Gordon, Thesis, Departament of Metallurgy, Massachusetts Institute of Technology, 1949.

14. S.T. Lin and R.E. Ogilvie, *J. Appl. Phys.* **34** (1963) 1372.

15. T. Shikama, A. Ochiai, and K. Susuki, *Proc. 4th Int. Symp. On Advances Nuclear Energy Research* (1992) 173.

16. Y. Haga, E. Yamamoto, N. Kimura, M. Hedo, H. Ohkuni, and Y. Onuki, *J. Magn. Magn. Mater.* **177-181** (1998) 437.

17. L. Lutterotti, P. Scardi, and P. Maistreli, *J. Appl. Cryst.* **25** (1992) 459.

18. B.D. Cullity, *Elements of X-Ray Diffraction*, 2ed. (Addison-Wesley, Mass., 1978) p. 377.

19. S.V. Vonsovsky, Y.A. Izyumov, and E.Z. Kurmaev, *Superconductivity in transition Metals* (Springer, New York, 1982) p. 234.

20. B.T. Matthias, V.B. Compton, H. Suhl, and E. Corenzwit, *Phys. Rev.* **115** (1959) 1597.